

Phase compensation method for Laguerre-Gaussian beam

HAOTIAN SHI^{1,2}, FANGFEI WU^{1,2}, HUIFENG ZHENG¹, XIAOYUE WANG^{1,*}, YANI ZUO^{2,*}

¹*China Jiliang University, Hangzhou 310018, China*

²*Division of Time and Frequency Metrology, National Institute of Metrology, Beijing 100029, China*

We propose a phase compensation method to deal with the phase twist of Laguerre-Gaussian (LG) beam. Theoretical analysis of the electric field expression allows the separation of the exponential term responsible for phase twist. For LG beam and a certain propagation distance, phase compensation is modulated and applied to the initial beam. Numerical calculations were conducted, comparing the evolution of LG beam without phase compensation and that with compensation. The compensation method effectively addresses the problem of phase twist during the transmission of LG beams, offering significant value for fields such as communication, imaging, and quantum sensing.

(Received March 25, 2025; accepted December 2, 2025)

Keywords: Laguerre beam, Orbital angular momentum, Phase compensation, Propagation characteristics

1. Introduction

Laguerre-Gaussian (LG) beam is a typical vortex beam, which has spiral phase profile and orbital angular momentum (OAM) [1–3]. The methods for effectively generating an LG beam are to direct a Gaussian beam onto a phase plate or spatial light modulator, and the emitted beam is the LG beam [4–6]. LG beam is widely used in the fields of communication, imaging and quantum sensing [7–9]. OAM rotates around the propagation axis, with the phase factor related to the topological charge l [10–12]. The topological charge plays a significant role in the generation, transmission, and dynamics of vortex light fields.

In recent years, many research works paid attention around the LG beam. Liu et al. demonstrated the generation of perfect optical vortices using LG beams, emphasizing the stability of their properties [13]. The study also extended the method to vector beams and explores applications in optical tweezers and high-capacity communications. Rasouli et al. presented a robust experimental method for characterizing LG beams using diffraction patterns, which simplifies the analysis of beam topological charge and radial index [14]. Both experimental and simulation results confirmed the accuracy and efficiency of the method. Kotlyar et al. theoretically demonstrated that the total topological charge of superposed LG beams equals the charge of individual beams under specific conditions [15]. Phase delays between beams can alter the total topological charge. Pan et al. investigated the mode purity of Gaussian vortex beams modulated by spiral phase plates [16]. The finding suggested that LG beams with lower topological charges maintain higher mode purity during propagation. Luo explored twisted anisotropic electromagnetic LG beams, revealing that manipulating beam anisotropy, topological

charge, and twist factor allows for engineering unique coherence and polarization patterns [17]. These findings had implications for fields like optical communications. Kotlyar et al. investigated the superposition of two LG beams, deriving relationships for complex amplitude in the Fresnel diffraction zone [18]. The beams demonstrated unique properties that could be useful for information transmission and optical communication.

As mentioned above, extensive research on LG beams has been conducted from various perspectives, including mode stability, phase delay, non-local effects, and optical computing. However, it is generally assumed that the phase of vortex beams remains stable during transmission, and there has been little theoretical research on the transmission of beams over long distances. As the transmission distance increases, the phase of the LG beam undergoes distortion, making it difficult to distinguish the OAM. However, with the growing research on vortex beams in communication, imaging, and quantum sensing, the demand for long-distance transmission of vortex beams and the need for OAM transmission stability have increased. Therefore, maintaining the phase of LG beams after long-distance transmission is crucial.

To solve the problem of phase twist and indistinguishable OAM after the long-distance transmission of LG beams, we propose a phase compensation method for phase distortion over a specified transmission distance by modulating the initial beam. Starting with the physical principles of LG beams, the electronical field of LG beam during propagation is derived by the diffraction integral. The exponential term of phase twist is separated. Aiming at the phase twist term, we perform phase modulation on the initial beam to apply targeted compensation for the twisted phase. This approach ensures that, after transmission, the isophase lines remain straight, allowing for clear distinction of the

OAM. Simulations of LG beams with various parameters were then performed, confirming the effectiveness of the phase compensation method proposed in this study. This method is also applicable to cases involving negative topological charges. The approach outlined in this paper advances the development of LG beams in fields such as communication, imaging, and quantum sensing, with significant implications for both theoretical and practical applications of vortex beams.

2. Theoretical analysis of LG beam

This section describes the theoretical analysis of LG beam. First, the propagation characteristic of LG beam is introduced. Then, the phase compensation method is explained.

LG beam is a typical vortex beam. By modulating the input Gaussian beam by a phase plate or spatial light modulator, the output beam becomes a LG beam. At the cross-section plane where the transmission distance is zero, the electric field of the LG beam in the cylindrical coordinate system (r, Φ) is

$$E(x, y, z) = \frac{-ikE_0}{2\pi z} \exp(ikz) \exp\left[\frac{ik(x^2 + y^2)}{2z}\right] \iint \exp\left[\left(\frac{ik}{2z} - \frac{1}{\omega_0^2}\right)(x_0^2 + y_0^2) - ik \frac{xx_0 + yy_0}{z}\right] \left(\frac{x_0 + iy_0}{\omega_0}\right)' dx_0 dy_0 \quad (3)$$

where x_0 and y_0 are the coordinates on the initial plane, and x and y are the coordinates on the plane with propagation distance of z .

$$E(x, y, z) = \frac{-ikE_0}{2\pi z} \exp(ikz) \exp\left[\frac{ik(x^2 + y^2)}{2\omega_0^2 \left(\frac{ik}{2z} - \frac{1}{\omega_0^2}\right)^2 z}\right] \iint \exp\left[-\left(\frac{ik}{2z} - \frac{1}{\omega_0^2}\right)^2 (X^2 + Y^2)\right] \left\{ \frac{X + iY + k(y - ix)/\left[2\left(\frac{ik}{2z} - \frac{1}{\omega_0^2}\right)^2 z\right]}{\omega_0} \right\}^l dX dY \quad (4)$$

Performing the integration of the Eq. (4), we obtain

$$E(x, y, z) = -iE_0 \left[\frac{k}{2} \left(\frac{ik}{2z} - \frac{1}{\omega_0^2} \right)^2 z \right]^{l+1} \left(\frac{y - ix}{\omega_0} \right)^l \exp(ikz) \exp\left[\frac{ik(x^2 + y^2)}{2\omega_0^2 \left(\frac{ik}{2z} - \frac{1}{\omega_0^2}\right)^2 z}\right] \quad (5)$$

Eq. (5) is the analytic expression of the electronic field of LG beam after the propagation distance z . By changing the value of topologic charge, we can the propagation evolution of LG beams of any order.

$$E(r, z) = E_0 (-i)^{l+1} \left(\sqrt{1 + \frac{4z^2}{k^2 \omega_0^4}} \right)^l \exp\left[-\frac{r^2}{\omega_0^2 \left(1 + \frac{4z^2}{k^2 \omega_0^4}\right)}\right] \exp(il\phi) \exp\left[ikz + \frac{i \cdot 2zr^2}{k \omega_0^4 \left(1 + \frac{4z^2}{k^2 \omega_0^4}\right)}\right] \quad (6)$$

From the first exponential term in Eq. (6), it can be observed that as the transmission distance increases, the beam size expands due to diffraction. The second

$$E_{z=0}(r, 0) = E_0 \left(\frac{r}{\omega_0} \right)^l \exp\left(\frac{-r^2}{\omega_0^2}\right) \exp(il\phi) \quad (1)$$

where E_0 is the normalized electric field strength coefficient, ω_0 is the size of the input beam, l is the topological charge.

From the perspective of the transmission direction, the beam consists of rays diverging from the transmission origin. From the cross-section plane along the transmission direction, the isophase surfaces of the LG beam exhibit a spiral structure. According to the diffraction integral, the electric field $E(r, z)$ at a transmission distance of z is

$$E(r, z) = \frac{-ik}{2\pi z} \exp(ikz) \iint E_{z=0}(r_0, 0) \exp\left[\frac{ik}{2z}(r - r_0)^2\right] dr \quad (2)$$

where k is the wave number.

Transform Eq. (2) into the Cartesian coordinate system, expressed as

Let $X = x_0 + ikx/[2z(1/\omega_0^2 - ik/2z)]$, $Y = y_0 + iky/[2z(1/\omega_0^2 - ik/2z)]$, Eq. (3) is transformed as

$$E(x, y, z) = \frac{-ikE_0}{2\pi z} \exp(ikz) \exp\left[\frac{ik(x^2 + y^2)}{2\omega_0^2 \left(\frac{ik}{2z} - \frac{1}{\omega_0^2}\right)^2 z}\right] \left\{ \frac{X + iY + k(y - ix)/\left[2\left(\frac{ik}{2z} - \frac{1}{\omega_0^2}\right)^2 z\right]}{\omega_0} \right\}^l dX dY \quad (4)$$

We transform Eq. (2) into an expression similar to Eq. (2), as

exponential term illustrates the topologic charge remains the same as the beam propagates. However, the third exponential term shows that the phase distribution changes

after propagation. This leads to phase twist. As the topological charge of the initial vortex beam changes and the transmission distance increases, the phase becomes indistinguishable as the distance increase. This results in the inability to identify the topological charge. Phase twist during vortex beam transmission poses a significant obstacle to research and applications in communication, imaging, and sensing.

$$E(r, z) = E_0(-i)^{l+1} \left(\sqrt{1 + \frac{4z^2}{k^2 \omega_0^4}} \right)^l \exp \left[-\frac{r^2}{\omega_0^2 \left(1 + \frac{4z^2}{k^2 \omega_0^4} \right)} \right] \exp(il\phi) \exp[ikz + \frac{i \cdot 2\pi r^2}{k\omega_0^4 \left(1 + \frac{4z^2}{k^2 \omega_0^4} \right)}] \exp[-ikZ - \frac{i \cdot 2\pi r^2}{k\omega_0^4 \left(1 + \frac{4Z^2}{k^2 \omega_0^4} \right)}]$$

The fourth exponential term is the phase compensation term. It compensates the total phase twist of the LG beam propagating during the distance Z . In this way, the beam gets phase compensation, and the phase twist is suppressed.

3. Results and discussions

This section primarily covers two aspects: the first is the numerical calculation of the phase twist of LG beams, and the second is the simulation of LG beams after phase compensation.

3.1. Phase twist of LG beam

We perform the simulation with the parameters: Gaussian beam size $\omega_0=10$ mm, wavelength $\lambda=532$ nm, propagation $d=100$ m, topologic charge $l=3$. The initial intensity profile and phase profile are shown in Fig. 1(a) and (e). After propagating 100 m in air, the intensity

The transmission distance is known in many applications of vortex beams in communication, imaging, and sensing. To solve this problem, it is possible to perform phase modulation on the initial LG beam. By compensating the phase, the beam can be transmitted to the target location with a distinguishable phase distribution. For a total transmission distance of Z , after phase compensation, the electronic field as distance z is expressed as

$$E(r, z) = E_0(-i)^{l+1} \left(\sqrt{1 + \frac{4z^2}{k^2 \omega_0^4}} \right)^l \exp \left[-\frac{r^2}{\omega_0^2 \left(1 + \frac{4z^2}{k^2 \omega_0^4} \right)} \right] \exp(il\phi) \exp[ikz + \frac{i \cdot 2\pi r^2}{k\omega_0^4 \left(1 + \frac{4z^2}{k^2 \omega_0^4} \right)}] \exp[-ikZ - \frac{i \cdot 2\pi r^2}{k\omega_0^4 \left(1 + \frac{4Z^2}{k^2 \omega_0^4} \right)}] \quad (7)$$

profile and phase are shown in Fig. 1(b) and (f). LG beams have significant research and application value in fields such as optical communication, optical computing, and quantum sensing. Their advantage lies in possessing orbital angular momentum, with the phase factor expressed as $\exp(il\Phi)$, where l is the topological charge. In experiments, the phase is measured using interference methods, and the light field distribution of an LG beam exhibits a doughnut structure, with a singularity at the center, where the light intensity forms a dark region. As a result, it is not possible to effectively measure the phase at the center, and only the phase in regions of higher intensity can be measured. In the simulation shown in Fig. 1(b) and (f), it can be observed that the topological charge at the center of the phase map can be distinguished; however, the overall phase distribution appears distorted, with isophase lines spiraling clockwise. This distortion is highly detrimental to assessing the topological charge of LG beams after long-distance transmission.

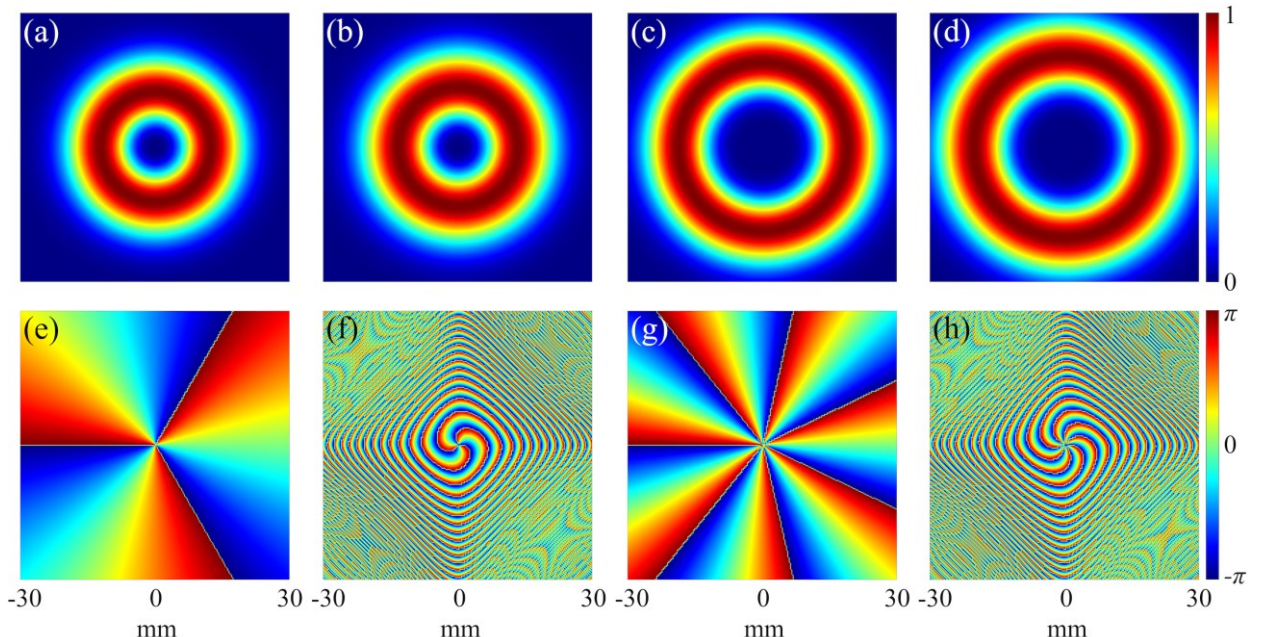


Fig. 1. Intensity profile of: (a) $l=3$, $z=0$ m; (b) $l=3$, $z=100$ m; (c) $l=7$, $z=0$ m; (d) $l=7$, $z=100$ m. Phase profile of: (a) $l=3$, $z=0$ m; (b) $l=3$, $z=100$ m; (c) $l=7$, $z=0$ m; (d) $l=7$, $z=100$ m (colour online)

For LG beams with a larger topological charge, $l = 7$, and the other input beam parameters remain the same, the initial light intensity profile and phase profile are shown in Fig. 1(c) and (g). After traveling 100 m in air, the intensity and phase profile are depicted in Fig. 1(d) and (h). As the topological charge increases, the intensity dark region at the center of the beam becomes larger. Additionally, with the increase in topological charge, the isophase lines become more densely packed, and the phase distortion becomes more severe as the transmission distance increases. Therefore, there is an urgent need to investigate a method to resolve the issue of phase twist and the inability to distinguish the topological charge after long-distance transmission of LG beams.

3.2. Phase compensation

Based on the phase compensation method in section 2, we perform the simulation. For the input LG beam with the topological charge of 3, the simulation parameters are: Gaussian beam size $\omega_0=10$ mm, wavelength $\lambda=532$ nm, propagation $d=100$ m. The beam intensity profiles at 0 m, 20 m, 40 m, 60 m, 80 m, 100 m are shown in Fig. 2(a-f). The cross-sectional intensities are depicted in Fig. 2(g-l). The phase distributions are illustrated in Fig. 2(m-r). From the intensity profile, as the transmission distance increases, the beam size also gradually increases. Fig. 2(m) shows the phase compensation on the initial LG beam, which has counterclockwise spiraling isophase lines. After transmission during 0 m to 100 m in air, the spiral structure of the isophase lines gradually unwinds, and the isophase lines change to straight lines, which is easy to distinguish the topological charge after 100-m propagation.

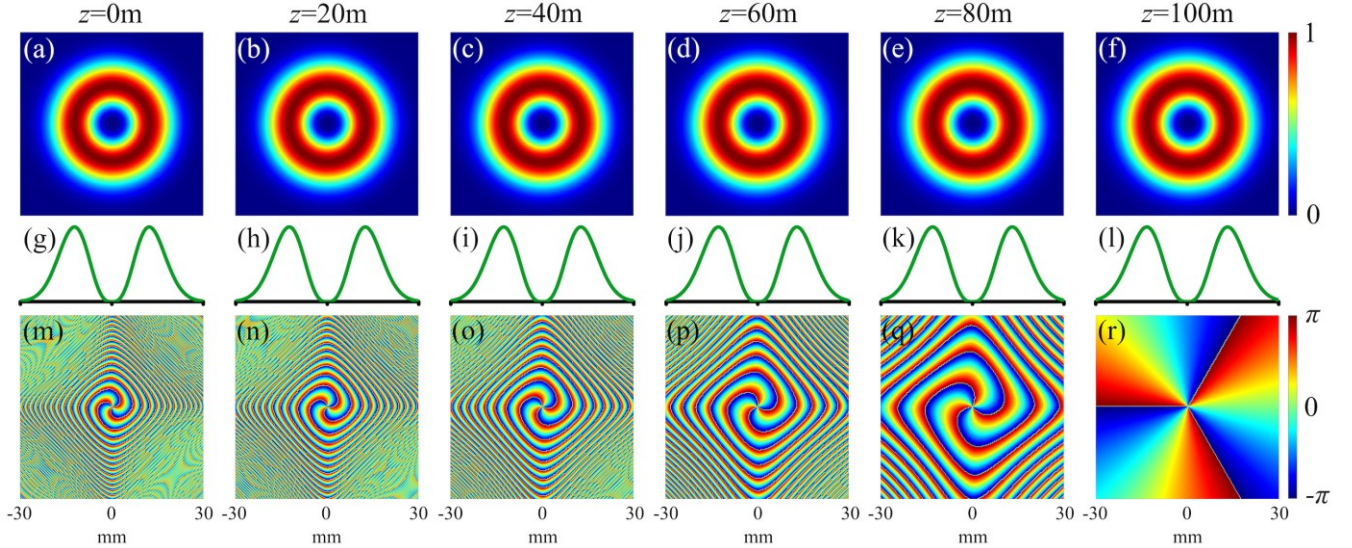


Fig. 2. Intensity profile of: (a) $l=3$, $z=0$ m; (b) $l=3$, $z=20$ m; (c) $l=3$, $z=40$ m; (d) $l=3$, $z=60$ m; (e) $l=3$, $z=80$ m; (f) $l=3$, $z=100$ m. Cross-section intensity profile of: (g) $l=3$, $z=0$ m; (h) $l=3$, $z=20$ m; (i) $l=3$, $z=40$ m; (j) $l=3$, $z=60$ m; (k) $l=3$, $z=80$ m; (l) $l=3$, $z=100$ m. Phase profile of: (m) $l=3$, $z=0$ m; (n) $l=3$, $z=20$ m; (o) $l=3$, $z=40$ m; (p) $l=3$, $z=60$ m; (q) $l=3$, $z=80$ m; (r) $l=3$, $z=100$ m (colour online)

Furthermore, we perform the simulation of the beam with larger topological charge of 7 and shorter propagation distance, to explore the evolution of beam propagation. The simulation parameters are: Gaussian beam size $\omega_0=1$ mm, wavelength $\lambda=532$ nm, propagation $d=1$ m. The simulation results are shown in Fig. 3. The beam intensity profiles at 0 m, 0.5 m, 0.9 m, 0.99 m, 0.999 m, 1 m are shown in Fig. 3(a-f). The cross-sectional intensities are depicted in Fig. 2(g-l). The phase distributions are illustrated in Fig. 3(m-r). From the intensity profile, as the transmission distance increases, both the beam size and the

width of the light ring gradually increase. Fig. 3(m) shows the phase compensation on the initial LG beam, in which the isophase lines rotate counterclockwise around the optical axis. From Fig. 3(m) to (f), the revolution of the phase distribution shows the effect of phase compensation. Phase profile with larger topological charge is more twisted and complicated. As the propagation distance increases, the twisted phase is alleviated, and the isophase lines change from curves to straight lines, which is of great significance for accurately identifying the topological charge and orbital angular momentum.

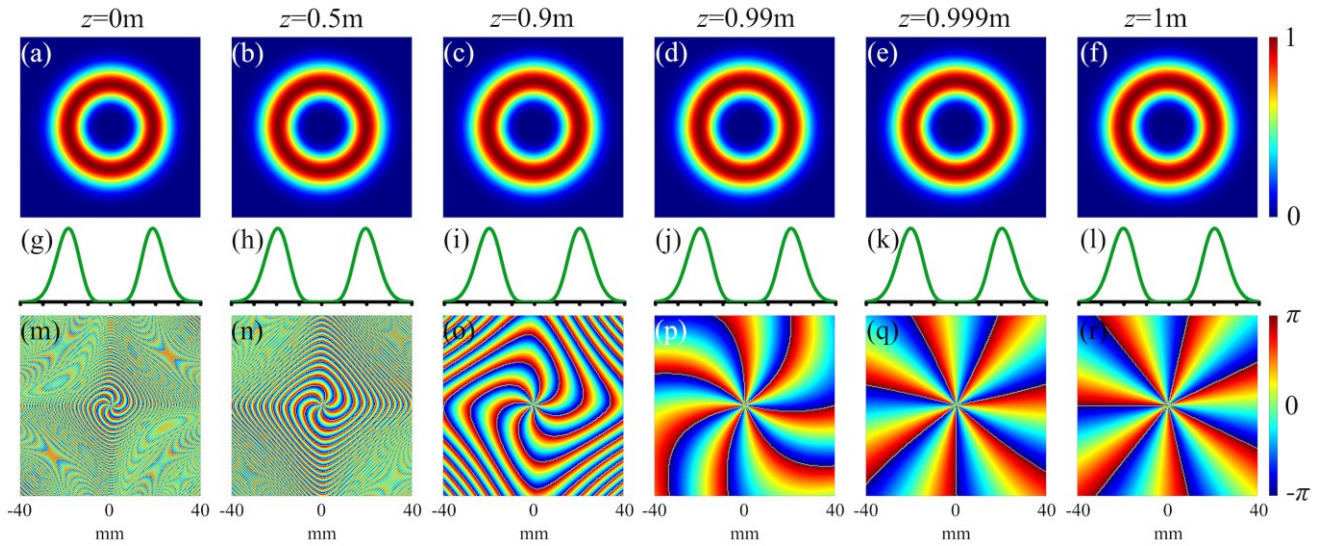


Fig. 3. Intensity profile of: (a) $l=7$, $z=0$ m; (b) $l=7$, $z=0.5$ m; (c) $l=7$, $z=0.9$ m; (d) $l=7$, $z=0.99$ m; (e) $l=7$, $z=0.999$ m; (f) $l=7$, $z=1$ m. Cross-section intensity profile of: (g) $l=7$, $z=0$ m; (h) $l=7$, $z=0.5$ m; (i) $l=7$, $z=0.9$ m; (j) $l=7$, $z=0.99$ m; (k) $l=7$, $z=0.999$ m; (l) $l=7$, $z=1$ m. Phase profile of: (m) $l=7$, $z=0$ m; (n) $l=7$, $z=0.5$ m; (o) $l=7$, $z=0.9$ m; (p) $l=7$, $z=0.99$ m; (q) $l=7$, $z=0.999$ m; (r) $l=7$, $z=1$ m (colour online)

The method proposed in this paper can be applied not only to positive topological charges but also extended to cases with negative topological charges. Compared to positive topological charges, negative topological charges give the phase an opposite spiral structure. In this section, we perform simulations of the LG beam evolution before and after phase compensation. LG beams experience phase distortion after long-distance transmission, making it impossible to distinguish the OAM. This is unacceptable for research and applications of vortex beams in fields such as communication, imaging, and quantum sensing. This paper proposes a phase compensation method based on the physical significance of LG beams, modulating, and compensating the phase of the emitted beam. The feasibility of this method has been verified through simulations, demonstrating that the LG beam can maintain a clear phase structure and distinguishable OAM even after long-distance transmission. This holds significant importance for research in cutting-edge physical technologies.

4. Conclusions

To address the issue of phase distortion and indistinguishable OAM after long-distance transmission of LG beams, this paper, based on the physical principles of LG beams, compensates for the phase twist over a specific transmission distance by modulating the initial beam. This ensures that, after transmission, the isophase lines remain straight, and the OAM can be clearly distinguished. Subsequently, simulations of LG beams with different parameters were conducted, and the results validated the effectiveness of the phase-compensation method proposed in this paper. This method can also be extended to cases with negative topological charges. The approach presented

in this paper promotes the development of LG beams in research areas such as communication, imaging, and quantum sensing, and has significant implications for both the theory and application of vortex beams.

Funding

This work was supported by the National Key R&D Program of China (Grant No. 2021YFF0603800), National Natural Science Foundation of China (Grant No.1230030120), the Natural Science Foundation of Zhejiang Province (Grant No. LQ24A040005, LQ24F050006), and the Fundamental Research Funds for the Provincial Universities of Zhejiang (Grant No. 2023YW54, 2023YW62).

Disclosures

The authors declare no conflicts of interest.

Data availability

Data underlying the results presented in this paper are not publicly available at this time but may be obtained from the authors upon reasonable request.

References

- [1] A. O. Pogrebnyaya, A. F. Rybas, *J. Opt. Technol.* **83**, 586 (2016).
- [2] J. Mendoza-Hernández, M. Hidalgo-Aguirre, A. Inclán Ladino, D. Lopez-Mago, *Opt. Lett.* **45**, 5197 (2020).
- [3] A. Luski, Y. Segev, R. David, O. Bitton, H. Nadler, A. Barnea, A. Gorlach, O. Cheshnovsky, I. Kaminer, E. Narevicius, *Science* **373**, 1105 (2021).

- [4] Y. Yang, Y. Li, C. Wang, *J. Opt.* **51**, 910 (2022).
- [5] M. Wang, Y. Ma, Q. Sheng, X. He, J. Liu, W. Shi, J. Yao, T. Omatsu, *Opt. Express* **29**, 27783 (2021).
- [6] C. Wang, Y. Chen, J. Wang, X. Yang, H. Gao, F. Li, *Front. Phys.* **19**, 42205 (2024).
- [7] A. Minoofar, X. Su, H. Zhou, R. Zhang, F. Alishahi, K. Zou, H. Song, K. Pang, S. Zash, M. Tur, A. Molisch, H. Sasaki, D. Lee, A. Willner, *J. Lightwave Technol.* **40**, 3285 (2022).
- [8] Y. Kozawa, R. Sakashita, Y. Uesugi, S. Sato, *Opt. Express* **28**, 18418 (2020).
- [9] J. Béguin, J. Laurat, X. Luan, A. P. Burgers, Z. Qin, H. Kimble, *Proc. Natl. Acad. Sci. U.S.A.* **117**, 26109 (2020).
- [10] K. Y. Bliokh, *Phys. Rev. Lett.* **126**, 243601 (2021).
- [11] K. Zhang, Y. Wang, Y. Yuan, S. N. Burokur, *Applied Sciences* **10**, 1015 (2020).
- [12] A. A. Kovalev, V. V. Kotlyar, A. P. Porfirev, *J. Opt. Soc. Am. A* **37**, 1740 (2020).
- [13] X. Liu, Y. Monfared, R. Pan, P. Ma, Y. Cai, C. Liang, *Applied Physics Letters* **119**, 021105 (2021).
- [14] S. Rasouli, S. Fathollazade, P. Amiri, *Opt. Express* **29**, 29661 (2021).
- [15] V. V. Kotlyar, A. A. Kovalev, P. Amiri, P. Soltani, S. Rasouli, *Opt. Express* **29**, 42962 (2021).
- [16] X. Pan, J. Wu, Z. Li, C. Zhang, C. Deng, Z. Zhang, H. Wen, Q. Gao, J. Yang, Z. Yi, M. Yu, L. Liu, F. Chi, P. Bai, *Optik* **230**, 166320 (2021).
- [17] M. Luo, D. Zhao, *Opt. Express* **28**, 31360 (2020).
- [18] V. V. Kotlyar, E. G. Abramochkin, A. A. Kovalev, A. A. Savelyeva, *Photonics* **9**, 496 (2022).

*Corresponding author: xywang_phy@163.com
zuoyn@nim.ac.cn